IOSR Journal of Electrical and Electronics Engineering (IOSR-JEEE)
e-ISSN: 2278-1676,p-ISSN: 2320-3331, Volume 10, Issue 1 Ver. III (Jan – Feb. 2015), PP 01-10
www.iosrjournals.org

Design, Modeling and Analysis of Linear Switched Reluctance Motor for Ground Transit Applications

[1]Praveen Kumar C, [2]K Geetha, [3]Madhavi K

Abstract: *Translations are the most common motions in several industrial branches. Usually the linear motion is generated by belt or spindle drives using rotational motors. Elasticity and backlash are the problems that hinder the accuracy of such drives. These mechanical arrangements provide low speed only. Utilization of high performance linear motors can eliminate these problems because they generate linear motion without any extra mechanical components. Linear switched reluctance motor (LSRM) is one of the linear motors that can be used in such drives. The design and mathematical modeling of a linear switched reluctance motor suitable for ground transit applications is presented in this paper.*

Key words: *LSRM, SRM, switched reluctance, flux linkage*

I. Introduction

The development of linear actuators is today a research field of interest to the field of engineering. Usually rotating to linear motion conversion is obtained through mechanical gears. Since this process is completely mechanical, a special maintenance is a must if high reliability and operational ability are demanded. Other drawbacks such as space or efficiency can be eliminated with the introduction of linear drives. Research is now focused on the invention of new materials and technologies with the ability to directly produce a linear displacement and, simultaneously, is also trying to solve issues related with linear actuators like the cogging force, the attractive force perpendicular to the motion [1]. A standard design procedure for a single-sided and longitudinal-flux-based linear switched reluctance machine (LSRM) is developed in [2], [5]. The proposed design procedure utilizes the rotating switched reluctance machine (rotary SRM) design by converting the specifications of the linear machine into those of an equivalent rotating machine. The machine design is carried out in the rotary domain, which then is transformed back into the linear domain. Linear machine drives combined with electromagnetic levitation are best suitable for conveyor applications in semiconductor fabrication plants and in low- and high speed transit applications because of their ability to produce propulsion force on the rotating part, known as the translator, without mechanical contact and friction. Linear switched reluctance machines (LSRMs) are the counterparts of the rotating switched reluctance machines. In fact, the linear switched reluctance machine is obtained from its rotary counterpart by cutting, along the shaft over its radius, both the stator and rotor and then rolling them out. A linear SRM may have windings either on the stator or translator (the moving part), whereas in the rotary switched reluctance machine the windings are always on the stator and the rotor contains no windings. The fixed part is called either a stator or track and the moving part is called a translator. There are two distinct configurations of linear SRM in the literature: longitudinal flux and transverse flux. These two configurations can be obtained by unrolling both the stator and rotor of a rotary SRM with a radial magnetic flux path and axial magnetic flux path, respectively. The converter topology with a minimum number of power devices and control implementations to facilitate the pulsation- free force control of the linear switched reluctance machines is investigated in [4]. Design of a high speed linear switched reluctance motor (LSRM) is presented in [6]. In [7], four longitudinal LSRM configurations are presented and designed to operate as propulsion actuators in a vertical elevator prototype. The most suitable LSRM configuration based on simplest construction, highest payload capability, and low copper loss, which is the modified high force density LSRM, is analyzed, designed, implemented, and tested as a propulsion actuator in a vertical elevator prototype. In [8], a self tuning regulator (STR) based on the pole placement algorithm is proposed for high-precision position tracking of the LSRM. A novel magnetic levitated switched reluctance linear actuator is proposed in [9]. The actuator is designed for applications in small to medium-scale automation machinery. The linear actuator has a simple and robust structure and is suitable for high-speed and high-precision position control with direct drive capability.

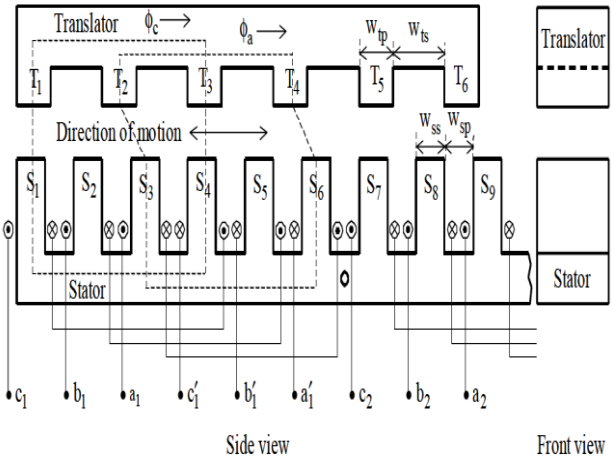

(a) Longitudinal Flux Path Configuration

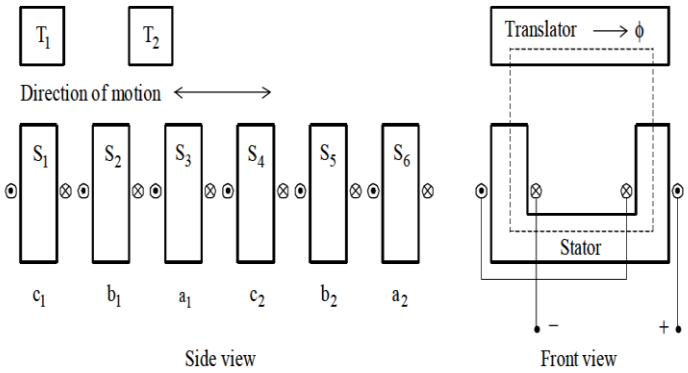

(b) Transverse Flux Path Configuration

Fig. 1 Three-Phase Linear LSRM with Active Stator and Passive Translator

II. Principle Of Operation

Linear switched reluctance machines (LSRMs) can be good alternative to linear induction or synchronous machines because of lack of windings on either the stator or rotor structure. Some of the features of these motors are:

- Lack of windings on either the stator or rotor structure.
- Absence of mechanical gears.
- Ideal for manufacturing and maintenance as the winding are concentrated.
- Windings are connected in series with a switch, so that the inductance of the winding can limit the rate of change of rising current, in case of a shoot through fault.
- The phases are independent and provide uninterrupted operation of the motor drives in the event of failure of one winding.
- Absence of significant heat sources during secondary operation and only one part of the secondary that is opposite to the primary is present in the magnetic field.

Some of the applications of LSRM are:

- Material handling systems.
- Transporting materials inside a totally enclosed system.
- Food processing plants, to move the items from one place to another.

A reluctance motor is an electric motor in which torque is produced by the tendency of its movable part to align to a position where the inductance of the excited winding is maximized. A switched reluctance motor (SRM) has simple construction compared to induction or synchronous machines. The structure of the switched reluctance motor constitutes a stator and a rotor as in the case of any other motor. The stator is composed of steel laminations shaped to form poles. The windings are always on the stator and rotor has no windings as shown in Fig.2. But a linear SRM may have windings either on the stator or translator. Longitudinal flux and transverse flux configurations for four-phase LSRM with an active translator and passive stator structure are

shown in Fig.1. The longitudinal magnetic flux path configuration is a linear counterpart of three-phase radial flux rotary SRM. The flux path in this machine is in the direction of the vehicle motion (Fig.1.a). A transverse flux design (Fig.1.b) has the flux path perpendicular to the direction of vehicle motion. It allows a simple track consisting of individually mounted transverse bars. As the flux is perpendicular to the direction of motion, an emf is induced in the core, resulting in high eddy current losses. If the stator is active and translator is passive, SRM configuration has the advantage of having the stationary power supply and power converters, resulting in reduced weight of the vehicle. But this design requires a large number of power converter sections along the track, resulting in high costs. When a pair of stator windings that are connected in series is excited, the translator tends to move so as to align itself with the magnetic flux axis of the excited stator phase windings. This position corresponds to the fully aligned position and has the maximum phase inductance. The position corresponding to maximum reluctance value and hence minimum phase inductance is called the unaligned position and occurs when a corresponding pair of translator poles that eventually will be aligned is half a translator pole pitch away from the axis of the excited stator poles. The translator moves forward smoothly when the stator windings are switched in sequence. According to the converter topology and the mode of operation, the previously excited phase may be turned off before or after the succeeding phase is excited. Reverse motion of the translator is achieved by reversing the excitation sequence of the stator phases.

The operation of the linear SRM depends on the inductance profile of the machine. The inductance of the machine depends on the machine dimensions such as the stator and translator pole and slot widths, excitation currents and translator position. The inductance characteristics are independent of stator current excitation since the magnetic circuit is assumed to be linear and using this, a relationship between the machine dimensions and inductance, shown in Fig.3, is derived.

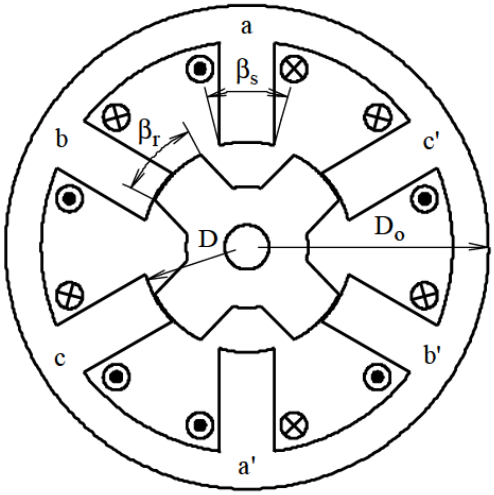

Fig. 2 Three Phase Rotary SRM

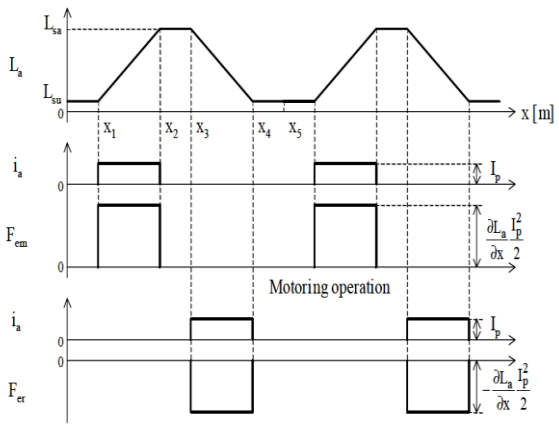

Fig. 3 Inductance Profile and Generation of Force of LSRM

The inductance of a phase winding is its self-inductance.
Five translator positions are significant to derive the inductance profile and they are given by,

$$x1 = \frac{Wts - Wsp}{2} \quad (1)$$

$$x2 = x1 + W_{sp}$$

$$x2 = \frac{Wts + Wsp}{2} \quad (2)$$

$$x3 = x2 + (Wtp - Wsp)$$

$$= Wtp + \left[\frac{Wts - Wsp}{2}\right] \quad (3)$$

$$= Wtp + \left[\frac{Wts + Wsp}{2}\right] \quad (4)$$

$$x4 = x3 + Wsp$$

$$x5 = x4 + \frac{Wts - Wsp}{2} \quad (5)$$

$$= Wtp + Wts \quad (6)$$

Where Wtp is the width of translator pole, Wts is the width of the translator slot, Wsp is the width of the stator pole, and Wss is the width of the stator slot. Between x2 and x3, there is complete overlap between stator and translator poles, and inductance during this interval is a maximum which corresponds to the aligned value. Zero propulsion force is generated in this region since there is no change in the inductance in this region. But this flat inductance region is important to give time to commutate the current and hence to prevent the generation of a negative force. Flat-top inductance profile is due to the unequal stator and translator pole widths. The regions corresponding to 0 to x1and x4 to x5 have no overlap between stator and translator poles. These positions have the minimum phase inductance called as unaligned inductance. The rate of change of inductance is zero and hence these regions do not contribute to propulsion force production. The forward direction of motion of the translator is assumed to be positive when the phase excitation sequence is abc. For reverse direction of motion, the phase sequence is acb. One half of the back emf power is stored in the form of magnetic field energy in phase windings and the other half of back emf power (or air gap power) is converted to mechanical power output.

III. Modeling Of LSRM

Current is generated by the magnetic field in an electromagnet.

A. Energy Analysis

We know that the instantaneous voltage across the terminals of a single-phase SRM winding is related to the flux linked in the winding by

Faraday's law,

$$v = iR + \frac{d\varphi}{dt} \quad (7)$$

Where

v is the terminal voltage

i is the phase current

R is the motor resistance

φ is the flux linked by the winding

The flux linkage in a SRM varies as a function of rotor position, θ and the motor current i.

Thus the equation can be represented as:

$$v = iR + \frac{d\varphi}{di}\frac{di}{dt} + \frac{d\varphi}{d\theta}\frac{d\theta}{dt} \quad (8)$$

Where $\frac{d\varphi}{di}$ is defined as winding inductance L (θ, i), which is a function of rotor position and current. Multiplying each side of equation by the electrical current, i, gives an expression for the instantaneous power in an SRM.

$$vi = i^2R + i\frac{d\varphi}{dt} \quad (9)$$

$$= i^2R + \frac{d\varphi}{di}\frac{di}{dt} \quad (10)$$

The left hand side of the equation represents the electrical power, delivered to the SRM. The first term on the right hand side represents the ohmic losses and the second term represents the electric power at coil terminal, which is a sum of mechanical output and any power stored in SRM.

$$P_e = L\frac{di}{dt}I \quad (11)$$

The relation between power and energy is,

$$\frac{dW_e}{dt} = P_e \quad (12)$$

Where W_e is a part of the total energy delivered to the winding, which is a sum of energy stored in the coil W_f and energy converted into mechanical work, W_m . It can be written as:

$$W_e = W_f + W_m \quad (13)$$

The magnetic field energy W_f can be given by the equation,

$$W_f = \int_0^{\varphi} id\varphi \quad (14)$$

The graphical interpretation of the field energy is shown in the Fig.5. The energy stored in the magnetic field with the air gap g, can be expressed in terms of magnetic flux density B_g as follows,

$$W_f = \int \frac{B_g}{\mu_o} dB_g V_{g=} \frac{B_g}{2\mu_o} V_g \quad (15)$$

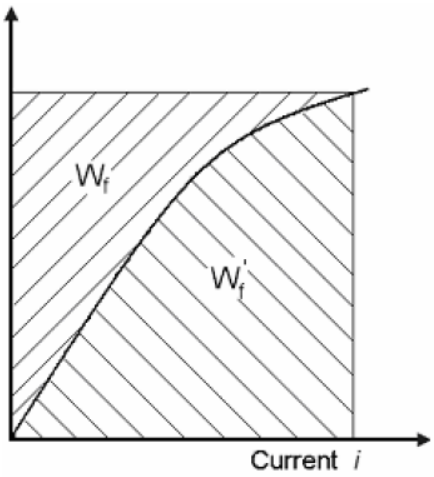

Fig. 4 Graphical Interpretation of Magnetic Field Energy

The field energy is inversely proportional to permeability and directly proportional to volume of air gap.
The area below the curve in Fig.5 is defined as magnetic Co- field energy. Co- field energy W_f' is defined by

$$W_f' = \int_0^i \varphi di \quad (16)$$

If $\varphi - i$ is non linear then $W_f' > W_f$. If $\varphi - i$ characteristic is linear then $W_f' = W_f$.
If the secondary part has moved slowly the current, i= v/R remains the same at both positions in the steady state because the coil resistance does not change and the voltage is set to be constant.

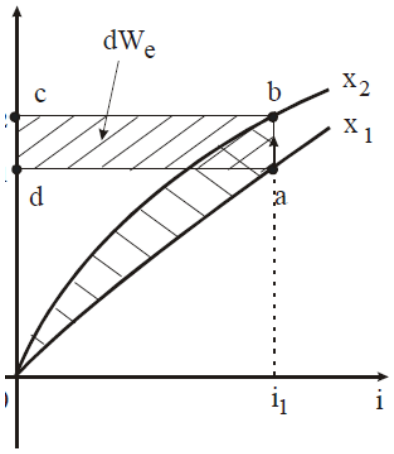

Fig. 5 Illustration to magnetic force derivation

The operating point has moved upward from point a to b (Fig.6).

B. Calculation of Force

The forces in the x, z, and y directions, named as the propulsion force, normal force, and lateral force, respectively, and shown in Fig. 6 is calculated using the principle of conservation of energy expressed as,

$$dW_i = dW_l + dW_s + dW_m \quad (17)$$

where dW_i is the incremental electric input energy, dW_l is the incremental loss energy dissipated by heat, dW_s is the incremental stored magnetic energy, and dW_m is the incremental mechanical energy. Assuming that the translator moves in x direction by da, the incremental mechanical energy is defined as,

$$dW_{ma} = f_a \times da \quad (18)$$

where f_a is the propulsion force generated. The same expression is used if appropriate

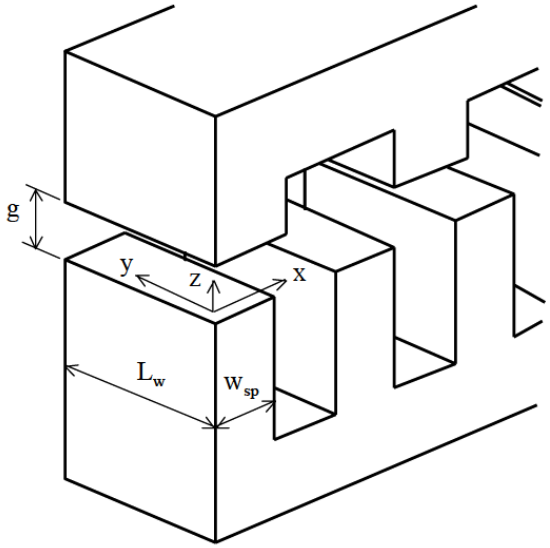

Fig. 6 Analytical Force Calculation Using Conservation of Energy

Direction and the displacements in that direction is for any other force. It is clear from the conservation of energy principle that the force calculations in x, z, and y directions require incremental values of electric input energy, loss energy dissipated by heat, and stored energy in the magnetic field.

The flux density in the air gap is given by,

$$\emptyset = \frac{B_g}{A\,B} \quad (19)$$

where A and B are the overlapped lengths in a particular position of the translator with respect to the stator in the x and y directions, respectively. Assuming a large air gap in the linear machine structure, Equation 19 can be written as,

$$\emptyset = B_g.AB = \mu_0 H_g.AB = \mu_0 \frac{T_{ph}\,i}{C} A\,B \quad (20)$$

$$= T_{ph}\,i = \frac{\emptyset\,Z}{\mu_0\,A\,B} \quad (21)$$

$$dW_e = i\,d\lambda = i\,d(T_{ph}\,\emptyset) = T_{ph}\,i\,d\emptyset = \frac{\emptyset\,Z}{\mu_0\,A\,B} \quad (22)$$

The stored energy in the magnetic field Ws is,

$$W_s = \frac{B_g{}^2\,A\,B\,C}{2\,\mu_0} = \left(\frac{\emptyset}{A\,B}\right)^2 . \frac{A\,B\,C}{2\mu_0} = \frac{\emptyset^2 C}{2\mu_0 A\,B} \quad (23)$$

$$dW_{sa} = -\frac{\emptyset^2\,C}{2\mu_0\,A^2 B} da + \frac{\emptyset\,C}{\mu_0\,A\,B} d\emptyset \quad (24)$$

Ignoring incremental energy due to losses such as copper loss, core loss, and mechanical friction loss, the incremental mechanical energy dW_{ma} during the incremental displacement da can be written as,

$$dW_{ma} = dW_i - dW_{sa}$$

$$= \frac{\emptyset\,C}{\mu_0 A\,B} d\emptyset + \frac{\emptyset^2 C}{2\mu_0\,A^2 B} da - \frac{\emptyset\,C}{\mu_{0\,A\,B}} d\emptyset$$

$$= \frac{\emptyset^2 C}{2\mu_0\,A^2 B} da \quad (25)$$

From which the propulsion force is now obtained as,

$$f_a = \frac{dW_{ma}}{da} = \frac{\emptyset^2 C}{2\mu_0\,A^2 B} = \frac{(B_g A\,B)^2 C}{2\mu_0\,A^2 B} = \frac{B_g{}^2}{2\mu_0} A\,B \quad (26)$$

The incremental stored magnetic energy dW_{sc} during the incremental displacement dc, which is the cause of the normal force, is given by,

$$dW_{sc} = \frac{\emptyset^2 C}{2\mu_0\,A^2 B} dc + \frac{\emptyset C}{2\mu_0\,A^2 B} d\emptyset \quad (27)$$

Ignoring incremental energy due to losses, the incremental mechanical energy dW_{mc} during the incremental displacement dz can be written as,

$$dW_{mc} = dW_i - dW_{sc}$$
$$= \frac{\emptyset\, C}{\mu_0\, A\, B} d\emptyset - \frac{\emptyset^2}{2\mu_0\, AB} dc - \frac{\emptyset\, C}{\mu_0\, A\, B} d\emptyset$$
$$= -\frac{\emptyset^2}{2\mu_0\, AB} dc \qquad (28)$$

The normal force is then obtained as,

$$f_c = \frac{dW_{mc}}{dc} = -\frac{\emptyset^2}{2\mu_0\, AB} = -\frac{(B_g A\, B)^2}{2\mu_0\, AB}$$
$$= -\frac{{B_g}^2}{2\mu_0} A\, B \qquad (29)$$

$$f_b = \frac{{B_g}^2}{2\mu_0} A\, B \qquad (30)$$

In the prototype design described in with L_w = 57.75 mm, W_{sp} = 23.1 mm, g = 1 mm, and B_g = 1.122 T, the propulsion force due to excitation of a single pole is,

$$f_{a1} = \frac{{B_g}^2}{2\mu_0} BC \qquad (31)$$
$$= \frac{{B_g}^2}{2\mu_0} \times L_w\, g \qquad (32)$$
$$= 28.901 \text{ N}$$

The propulsion force due to the excitation of a phase is $f_a = 2 \times f_{a1} = 57.802$ N.

The normal force due to excitation of a single pole is calculated as,

$$f_{c1} = -\frac{{B_g}^2}{2\mu_0} A\, B \qquad (33)$$
$$= -\frac{{B_g}^2}{2\mu_0} W_{sp}\, L_w$$
$$= \text{-668.205 N}$$

The total downward force experienced by the translator is given by $f_c = 2 \times f_{c1} = -1336.41$ N.

The normal force can be calculated at different translator positions by changing the overlap length A.

Flux linkages in the machine are calculated for a given excitation and a translator position using magnetic equivalent circuit. The flux linkages can be obtained from the inductance and corresponding excitation current.

The magnetic flux path of an LSRM involves five parts of the machine, namely, air gaps, stator poles, stator yoke, translator poles, and translator yoke. Each part experiences different flux densities and different lengths of flux line based on the chosen magnetic flux path. The mmf applied to a phase winding at any translator position is given by equation 34.

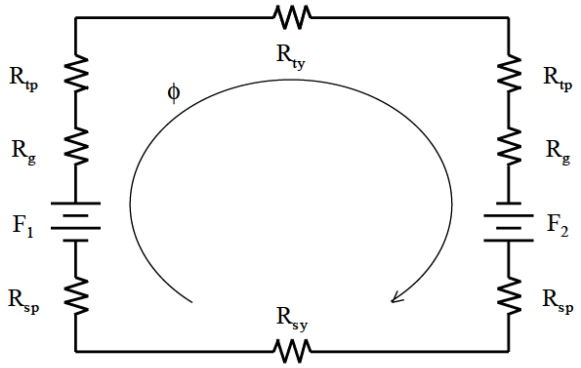

R_{tp}, R_{ty}: Reluctances of the translator pole and yoke
R_{sp}, R_{sy}: Reluctances of the stator pole and yoke
R_g: Reluctance of the air gap
F_1, F_2: Applied mmfs per pole, ϕ: Magnetic flux

Fig. 7 Lumped Parameter Model of Equivalent Magnetic Circuit of LSRM

$$F_P = F_1 + F_2 = F_{ag} + F_{st} + F_{tl} \qquad (34)$$

where F_P is the total mmf per phase applied, F_{ag}, F_{st}, and F_{tl} are the mmf drops in the air gap, stator iron core, and translator iron core, respectively.

The mmf equation can be rewritten in terms of the magnetic field intensity and flux path length using Ampere's Circuital Law as,

$$F_P = T_{ph}\, i = \Sigma\, H_{ag}\, l_{ag} + \Sigma\, H_{st}\, l_{st} + \Sigma\, H_{tl}\, l_{tl} \qquad (35)$$

where H_{ag}, H_{st}, H_{tl}, l_{ag}, l_{st}, and l_{tl} are the magnetic field intensities and flux path lengths in the air gap, stator iron core, and translator iron core, respectively.

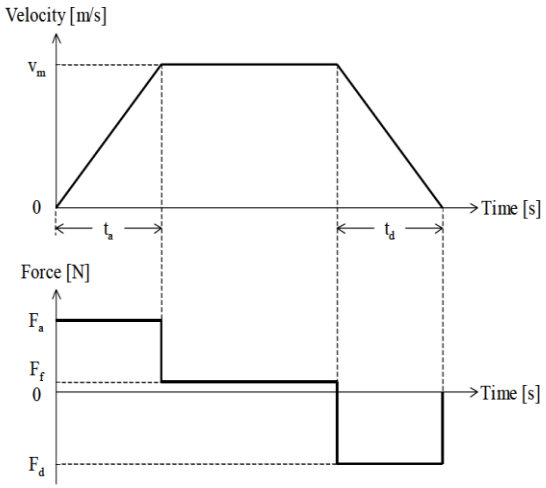

Fig. 8 Velocity and Required Force Profiles of LSRM

IV. Design Of A Prototype With Active Stator And Passive Translator

An LSRM prototype id designed for a length of 6 m, with a maximum linear velocity of 3 m/s and acceleration time of 1 second. The maximum mass of translator assembly is restricted to 20 kg.

Acceleration is given by,

$$a_a = \frac{V_m}{t_a} = 3\ m/s^2 \quad (36)$$

Force for initial acceleration is calculated as

$$F_a = M_t a_a = 60\ N \quad (37)$$

The deceleration, $a_d = -3 m/s^2$ and deceleration force F_d = - 60 N

Power capacity of LSRM is

$$P = F_a \times V_m = 180\ W \quad (38)$$

The RSRM is assumed to have a stator pole angle

β_s= 30° = 0.524 rads

Rotor pole angle β_r= 36°= 0.628 rads

K_e= 0.4, K_d= 1, K_2= 0.7, B_g= 1.1215 T

A_{sp}= 23886.5

K= 0.655

Bore diameter, $D = \sqrt{\frac{p\pi}{60\ Ke\ Kd\ K1\ K2\ Bg\ Asp\ Vm}}$ (39)

= 88.17 mm

Stack length of RSRM is

$$L = KD \quad (40)$$

= 57.75 mm

Stator yoke thickness, C_{sy} is given by

$$C_{sy} = \frac{D\,\beta_s}{2} = 23.1 mm \quad (41)$$

Assuming D_0= 190 mm, height of stator pole $h_s = \frac{D_0}{2} - \frac{D}{2} - C_{sy} = 27.815$ mm (42)

Rotor back iron width C_{ry} and the height of the rotor pole (translator pole) h_r are then calculated as,

$$C_{ry} = \left(\frac{D}{2}\right) \beta_r = 27.69\ mm \quad (43)$$

$$h_r = \frac{D}{2} - g - C_{ry} = 15.4\ mm \quad (44)$$

Magnetic field intensity in the air gap is calculated as,

$$H_g = \frac{B_g}{\mu_0} = 892461.3 A/m \quad (45)$$

For a peak phase current of I_p= 8.5 A,

Number of turns per phase is

$$T_{ph} = \frac{H_g\ 2g}{I_p} = 210\ turns/phase \quad (46)$$

Assuming a current density of J= 6 A/mm^2,

Area of conductor is,

$a_c = \frac{I_p}{J\sqrt{m}} = 0.818\ mm^2$ (47)

The closest wire size for this area of cross section of the conductor is AWG # 18 and it has an area of 0.817mm^2 and it is selected for the phase windings.

A. Conversion from RSRM to LSRM

The number of sectors of the LSRM and the resultant total number of stator poles are

$N_{sc} = \frac{L_t}{\pi D} = 22$ (48)

$n = N_s N_{sc} = 132$ (49)

Width of stator pole and width of stator slot are given by,

$W_{sp} = \frac{D\,\beta_s}{2} = 23.1mm$ (50)

$W_{ss} = \frac{\pi D - 6W_{sp}}{6} = 23.1\ mm$ (51)

Translator pole width and translator slot width are,

$W_{tp} = C_{ry} = 27.7\ mm$

$W_{ts} = \frac{\pi D - 4W_{tp}}{4} = 41.55\ mm$ (52)

Total length of the translator is given by,

$L_{tr} = 6W_{tP} + 5W_{ts} = 373.95\ mm$ (53)

The core stack width of the LSRM is obtained from stator stack length of RSRM as,

$L_w = L = KD = 57.75\ mm$

Diameter of the conductor is given by,

$$d_c = \sqrt{\frac{4a_c}{\pi}} = 1.02\ mm$$

Assuming width of wedges, w= 3 and packing factor, f_f = 0.8, number of vertical layers of winding and number of horizontal layers of winding are obtained as,

$N_v = f_f \frac{(h_s - w)}{d_c} = 20$ (54)

$N_h = \frac{T_{ph}}{2\,N_v} = 7$ (55)

Stator winding area is given by,

$\frac{2\,a_c\,N_v N_h}{f_f} = 286.3\ mm^2$ (56)

Fill factor is calculated as

$f_f = \frac{stator\ \ winding\ \ area}{stator\ \ slot\ \ window\ \ area} = 0.499$ (57)

Fill factor is in the range 0.2<= FF < 0.7

Finally, the following condition is to be satisfied.

$N_s(W_{sp} + W_{ss}) = N_t(W_{tp} + W_{ts})$ (58)

The duty cycle of a winding in the three-phase LSRM, 1/(3Nsc) whereas that of the RSRM winding it is 1/3. Therefore, the windings in the LSRM can have much lower copper volume but taking more losses.

V. Conclusion

A novel design procedure for linear switched reluctance machine was proposed using the current knowledge and design procedure of rotating switched reluctance machine**.** The force analysis of the prototype was also carried out. The principle of operation of the linear switched reluctance motor was described along with modeling.

Acknowledgement

We sincerely acknowledge with the financial support extended by Centre for Engineering Research and Development (CERD), Thiruvananthapuram for the execution of this project work.

About The Authors

Mr Praveen Kumar C is working as Assistant Professor in the Department of Electrical and Electronics Engineering at NSS College of Engineering, Palakkad, Kerala. He received the ME Degree in Mechatronics from Anna University in 2013. His areas of interest include Special Machines, Linear Machines and Jet propulsion.

Dr K Geetha is working as Professor in the Department of Electrical and Electronics Engineering at NSS College of Engineering, Palakkad, Kerala. She has around 32 years of teaching experience in various fields related to electrical and electronics. Her research interests include power electronics and drives and special machines.

Ms Madhavi K is pursuing her M Tech degree in Power Electronics at NSS College of Engineering, Palakkad. She is doing her Master Research Project in the area of Linear Switched Reluctance Machines.

References

[1]. Antonio Eduardo Victoria, Maria, Carlos Manuel Pereira, "Design and Evaluation of Linear Switched Reluctance Actuator For Positioning Tasks", Turk J Elec Eng & Comp Sci, Vol.18, No.6, 2010.

[2]. R Krishnan, Switched Reluctance Motor Drives: Modeling, Simulation, Analysis, Design, and Applications, 1st ed. Boca Raton, FL: CRC, 2001, pp.

[3]. Lee, Byeong-Seok, Han-Kyung Bae, Praveen Vijayraghavan, and R. Krishnan, "Design of a linear switched reluctance machine", in Conf. Rec. of the 1999 IEEE IAS Ann. Mtg., Oct. 1999, Phoenix, AZ, pp. 2267–2274.

[4]. Bae, Han-Kyung, Byeong-Seok Lee, Praveen Vijayraghavan, and R. Krishnan, "Linear switched reluctance motor: converter and control", in Conf. Rec. of the 1999 IEEE IAS Ann. Mtg., Oct. 1999, Phoenix, AZ, pp. 547–554.

[5]. B. S. Lee, "Linear switched reluctance machine drives with electromagnetic levitation and guidance systems." Ph.D. thesis, The Bradley Department of Electrical and Computer Engineering, Virginia Tech., Blacksburg, VA, November 2000.

[6]. Seok-Myeong Jang1, Ji-Hoon Park1, Dae-Joon You1, Han-Wook Cho1, Ho-Kyung Sung "Design of High Speed Linear Switched Reluctance Motor", Proceeding of International Conference on Electrical Machines and Systems 2007, Oct. 8~11, Seoul, Korea, pp. 1668-1671.

[7]. N. S. Lobo, Hong Sun Lim, R Krishnan, "Comparison of Linear Switched Reluctance Machines for Vertical Propulsion Application: Analysis, Design, and Experimental Correlation", IEEE Trans. on Ind. Applications, Vol. 44, No. 4, July/August 2008, Pp. 1134- 1142.

[8]. Shi Wei Zhao, Norbert C. Cheung, Wai-Chuen Gan, and Jin Ming Yang, "High-Precision Position Control of a Linear-Switched Reluctance Motor Using a Self-Tuning Regulator", IEEE Transactions on Power Electronics, Vol. 25, No. 11, November 2010, pp. 2820-2827.

[9]. Zhen Gang Sun, nobert C Chung, Shi Wei Zhao, and Wai- Chen Gan, "Magnetic analysis of switched reluctance actuators in levitated linear transporters", IEEE Trans. on Vehicular Technology, Vol.59, No.9, Nov.2010, pp.4280- 4288.